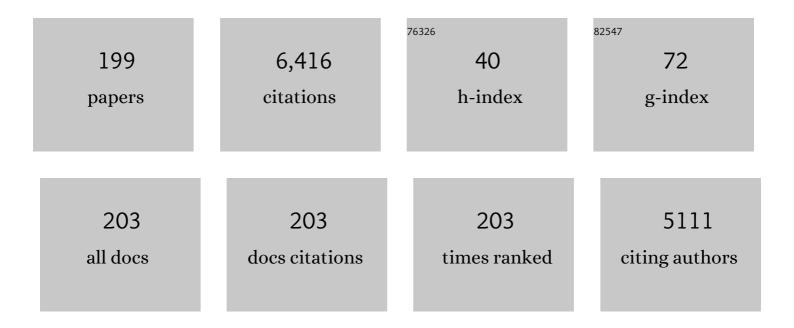
Jianlin Zhao

List of Publications by Year in descending order

Source: https://exaly.com/author-pdf/4606984/publications.pdf Version: 2024-02-01



ΙΙΔΝΙΙΝ ΖΗΔΟ

#	Article	IF	CITATIONS
1	WS2 mode-locked ultrafast fiber laser. Scientific Reports, 2015, 5, 7965.	3.3	406
2	One-step robust deep learning phase unwrapping. Optics Express, 2019, 27, 15100.	3.4	219
3	Anti–parity-time symmetry in diffusive systems. Science, 2019, 364, 170-173.	12.6	217
4	Nonlinear Saturable Absorption of Liquidâ€Exfoliated Molybdenum/Tungsten Ditelluride Nanosheets. Small, 2016, 12, 1489-1497.	10.0	211
5	WS_2 saturable absorber for dissipative soliton mode locking at 106 and 155 µm. Optics Express, 2015, 23, 27509.	3.4	187
6	Graphene-assisted all-fiber phase shifter and switching. Optica, 2015, 2, 468.	9.3	183
7	Chiralityâ€Assisted Highâ€Efficiency Metasurfaces with Independent Control of Phase, Amplitude, and Polarization. Advanced Optical Materials, 2019, 7, 1801479.	7.3	181
8	Erbium-doped fiber laser passively mode locked with few-layer WSe2/MoSe2 nanosheets. Scientific Reports, 2016, 6, 23583.	3.3	168
9	Interference-assisted kaleidoscopic meta-plexer for arbitrary spin-wavefront manipulation. Light: Science and Applications, 2019, 8, 3.	16.6	153
10	Generation of perfect vectorial vortex beams. Optics Letters, 2016, 41, 2205.	3.3	151
11	Passively Q-Switched and Mode-Locked Fiber Laser Based on an ReS2 Saturable Absorber. IEEE Journal of Selected Topics in Quantum Electronics, 2018, 24, 1-6.	2.9	144
12	Completely Spin-Decoupled Dual-Phase Hybrid Metasurfaces for Arbitrary Wavefront Control. ACS Photonics, 2019, 6, 211-220.	6.6	132
13	Label-free glucose biosensor based on enzymatic graphene oxide-functionalized tilted fiber grating. Sensors and Actuators B: Chemical, 2018, 254, 1033-1039.	7.8	121
14	Y-Net: a one-to-two deep learning framework for digital holographic reconstruction. Optics Letters, 2019, 44, 4765.	3.3	119
15	Graphene-supported manipulation of surface plasmon polaritons in metallic nanowaveguides. Photonics Research, 2017, 5, 162.	7.0	105
16	A highly efficient thermo-optic microring modulator assisted by graphene. Nanoscale, 2015, 7, 20249-20255.	5.6	99
17	A MoSe ₂ /WSe ₂ Heterojunctionâ€Based Photodetector at Telecommunication Wavelengths. Advanced Functional Materials, 2018, 28, 1804388.	14.9	95
18	Phase aberration compensation of digital holographic microscopy based on least squares surface fitting. Optics Communications, 2009, 282, 3873-3877.	2.1	91

#	Article	IF	CITATIONS
19	Generation of polarization and phase singular beams in fibers and fiber lasers. Advanced Photonics, 2021, 3, .	11.8	89
20	High-order optical vortex generation in a few-mode fiber via cascaded acoustically driven vector mode conversion. Optics Letters, 2016, 41, 5082.	3.3	87
21	Fullâ€Color Holographic Display and Encryption with Fullâ€Polarization Degree of Freedom. Advanced Materials, 2022, 34, e2103192.	21.0	85
22	All-optical control of microfiber resonator by graphene's photothermal effect. Applied Physics Letters, 2016, 108, .	3.3	81
23	Dual-wavelength common-path digital holographic microscopy for quantitative phase imaging based on lateral shearing interferometry. Applied Optics, 2016, 55, 7287.	2.1	76
24	Ultrafast all-fiber based cylindrical-vector beam laser. Applied Physics Letters, 2017, 110, .	3.3	69
25	Synchronized multi-wavelength soliton fiber laser via intracavity group delay modulation. Nature Communications, 2021, 12, 6712.	12.8	67
26	Strong plasmonic confinement and optical force in phosphorene pairs. Optics Express, 2017, 25, 5255.	3.4	65
27	Flexibly tunable high-quality-factor induced transparency in plasmonic systems. Scientific Reports, 2018, 8, 1558.	3.3	65
28	Recent progress of pulsed fiber lasers based on transition-metal dichalcogenides and black phosphorus saturable absorbers. Nanophotonics, 2020, 9, 2215-2231.	6.0	58
29	Extraordinary Second Harmonic Generation in ReS ₂ Atomic Crystals. ACS Photonics, 2018, 5, 3485-3491.	6.6	57
30	Chip-integrated van der Waals PN heterojunction photodetector with low dark current and high responsivity. Light: Science and Applications, 2022, 11, 101.	16.6	57
31	Second Harmonic Generation in Atomically Thin MoTe ₂ . Advanced Optical Materials, 2018, 6, 1701334.	7.3	54
32	Graphene-empowered dynamic metasurfaces and metadevices. Opto-Electronic Advances, 2022, 5, 200098-200098.	13.3	54
33	Quantitative phase microscopy for cellular dynamics based on transport of intensity equation. Optics Express, 2018, 26, 586.	3.4	53
34	Second Harmonic and Sum-Frequency Generations from a Silicon Metasurface Integrated with a Two-Dimensional Material. ACS Photonics, 2019, 6, 2252-2259.	6.6	52
35	Sb2Te3 topological insulator: surface plasmon resonance and application in refractive index monitoring. Nanoscale, 2019, 11, 4759-4766.	5.6	52
36	Magnetic plasmon resonances in nanostructured topological insulators for strongly enhanced light–MoS2 interactions. Light: Science and Applications, 2020, 9, 191.	16.6	52

#	Article	IF	CITATIONS
37	In-Line Mach-Zehnder Interferometer With D-Shaped Fiber Grating for Temperature-Discriminated Directional Curvature Measurement. Journal of Lightwave Technology, 2018, 36, 742-747.	4.6	49
38	Y4-Net: a deep learning solution to one-shot dual-wavelength digital holographic reconstruction. Optics Letters, 2020, 45, 4220.	3.3	49
39	High-efficiency second-order nonlinear processes in an optical microfibre assisted by few-layer GaSe. Light: Science and Applications, 2020, 9, 63.	16.6	44
40	Vortex-controlled morphology conversion of microstructures on silicon induced by femtosecond vector vortex beams. Applied Physics Letters, 2017, 111, .	3.3	44
41	High-performance humidity sensor based on a polyvinyl alcohol-coated photonic crystal cavity. Optics Letters, 2016, 41, 5515.	3.3	43
42	Fano resonance lineshapes in a waveguide-microring structure enabled by an air-hole. APL Photonics, 2020, 5, .	5.7	42
43	Catalystlike effect of orbital angular momentum on the conversion of transverse to three-dimensional spin states within tightly focused radially polarized beams. Physical Review A, 2018, 97, .	2.5	41
44	Topological insulator based Tamm plasmon polaritons. APL Photonics, 2019, 4, .	5.7	40
45	A compact structure for realizing Lorentzian, Fano, and electromagnetically induced transparency resonance lineshapes in a microring resonator. Nanophotonics, 2019, 8, 841-848.	6.0	40
46	Graphene Actively Mode‣ocked Lasers. Advanced Functional Materials, 2018, 28, 1801539.	14.9	39
47	Phase-matching-induced near-chirp-free solitons in normal-dispersion fiber lasers. Light: Science and Applications, 2022, 11, 25.	16.6	39
48	Transport of intensity equation from a single intensity image via deep learning. Optics and Lasers in Engineering, 2020, 134, 106233.	3.8	35
49	Mode evolution and nanofocusing of grating-coupled surface plasmon polaritons on metallic tip. Opto-Electronic Advances, 2018, 1, 18001001-18001007.	13.3	35
50	Digital holographic interferometry based on wavelength and angular multiplexing for measuring the ternary diffusion. Optics Letters, 2012, 37, 1211.	3.3	34
51	Longitudinal spin separation of light and its performance in three-dimensionally controllable spin-dependent focal shift. Scientific Reports, 2016, 6, 20774.	3.3	33
52	High performance graphene oxide-based humidity sensor integrated on a photonic crystal cavity. Applied Physics Letters, 2017, 110, .	3.3	33
53	Tunable nonreciprocal reflection and its stability in a non-PT-symmetric plasmonic resonators coupled waveguide systems. Applied Physics Express, 2020, 13, 012009.	2.4	33
54	Quasi-Bessel beams with longitudinally varying polarization state generated by employing spectrum engineering. Optics Letters, 2016, 41, 4811.	3.3	32

Jianlin Zhao

#	Article	IF	CITATIONS
55	Automatic compensation of phase aberrations in digital holographic microscopy based on sparse optimization. APL Photonics, 2019, 4, .	5.7	32
56	2D materials-enabled optical modulators: From visible to terahertz spectral range. Applied Physics Reviews, 2022, 9, .	11.3	32
57	Au–InSe van der Waals Schottky junctions with ultralow reverse current and high photosensitivity. Nanoscale, 2020, 12, 4094-4100.	5.6	31
58	Tying Polarizationâ€Switchable Optical Vortex Knots and Links via Holographic Allâ€Dielectric Metasurfaces. Laser and Photonics Reviews, 2020, 14, 1900366.	8.7	31
59	Controllable oscillated spin Hall effect of Bessel beam realized by liquid crystal Pancharatnam-Berry phase elements. Light: Science and Applications, 2022, 11, .	16.6	31
60	Graphene-controlled fiber Bragg grating and enabled optical bistability. Optics Letters, 2016, 41, 603.	3.3	30
61	RestoreNet: a deep learning framework for image restoration in optical synthetic aperture imaging system. Optics and Lasers in Engineering, 2021, 139, 106463.	3.8	30
62	Graphene-induced unique polarization tuning properties of excessively tilted fiber grating. Optics Letters, 2016, 41, 5450.	3.3	29
63	A method for simultaneously measuring polarization and phase of arbitrarily polarized beams based on Pancharatnam-Berry phase. Applied Physics Letters, 2017, 110, .	3.3	28
64	Bend measurement using an etched fiber incorporating a fiber Bragg grating. Optics Letters, 2013, 38, 214.	3.3	27
65	Highly efficient plasmonic nanofocusing on a metallized fiber tip with internal illumination of the radial vector mode using an acousto-optic coupling approach. Nanophotonics, 2019, 8, 921-929.	6.0	27
66	Resolution improvement of digital holographic images based on angular multiplexing with incoherent beams in orthogonal polarization states. Optics Letters, 2010, 35, 3519.	3.3	25
67	Observation of excitonic series in monolayer and few-layer black phosphorus. Physical Review B, 2020, 101, .	3.2	25
68	Improvement of measurement accuracy in digital holographic microscopy by using dual-wavelength technique. Journal of Micro/ Nanolithography, MEMS, and MOEMS, 2015, 14, 041313.	0.9	24
69	Common-path digital holographic microscopy for near-field phase imaging based on surface plasmon resonance. Applied Optics, 2017, 56, 3223.	2.1	24
70	Linear Dichroism and Nondestructive Crystalline Identification of Anisotropic Semimetal Few‣ayer MoTe ₂ . Small, 2019, 15, e1903159.	10.0	24
71	Valley Vortex States and Degeneracy Lifting via Photonic Higher-Band Excitation. Physical Review Letters, 2019, 122, 123903.	7.8	24
72	High capacity topological coding based on nested vortex knots and links. Nature Communications, 2022, 13, 2705.	12.8	24

#	Article	IF	CITATIONS
73	Quantitative measurement of thermal lensing in diode-side-pumped Nd:YAG laser by use of digital holographic interferometry. Optics Express, 2016, 24, 28185.	3.4	23
74	A review of common-path off-axis digital holography: towards high stable optical instrument manufacturing. Light Advanced Manufacturing, 2021, 2, 1.	5.1	23
75	Compact surface plasmon holographic microscopy for near-field film mapping. Optics Letters, 2017, 42, 3462.	3.3	22
76	Cylindrical vector beam-excited frequency-tunable second harmonic generation in a plasmonic octamer. Photonics Research, 2018, 6, 157.	7.0	22
77	MoTe ₂ PN Homojunction Constructed on a Silicon Photonic Crystal Cavity for High-Performance Photodetector. ACS Photonics, 2021, 8, 2431-2439.	6.6	22
78	Measurement of ultrafast combustion process of premixed ethylene/oxygen flames in narrow channel with digital holographic interferometry. Optics Express, 2018, 26, 28497.	3.4	21
79	Optical vortex fiber laser based on modulation of transverse modes in two mode fiber. APL Photonics, 2019, 4, .	5.7	20
80	Ultralow Threshold, Single-Mode InGaAs/GaAs Multiquantum Disk Nanowire Lasers. ACS Nano, 2021, 15, 9126-9133.	14.6	19
81	Complete structural characterization of single carbon nanotubes by Rayleigh scattering circular dichroism. Nature Nanotechnology, 2021, 16, 1073-1078.	31.5	18
82	Giant and Anisotropic Nonlinear Optical Responses of 1D van der Waals Material Tellurium. Advanced Optical Materials, 2020, 8, 2001273.	7.3	17
83	RestoreNet-Plus: Image restoration via deep learning in optical synthetic aperture imaging system. Optics and Lasers in Engineering, 2021, 146, 106707.	3.8	17
84	Acceleration of autofocusing with improved edge extraction using structure tensor and Schatten norm. Optics Express, 2020, 28, 14712.	3.4	17
85	Classification of cell morphology with quantitative phase microscopy and machine learning. Optics Express, 2020, 28, 23916.	3.4	17
86	Quantitative and Dynamic Phase Imaging of Biological Cells by the Use of the Digital Holographic Microscopy Based on a Beam Displacer Unit. IEEE Photonics Journal, 2018, 10, 1-10.	2.0	16
87	Self-accelerated optical activity in free space induced by the Gouy phase. Photonics Research, 2020, 8, 475.	7.0	16
88	Visual investigation on the heat dissipation process of a heat sink by using digital holographic interferometry. Journal of Applied Physics, 2013, 114, .	2.5	15
89	Multiple Optical Frequency Conversions in Few‣ayer GaSe Assisted by a Photonic Crystal Cavity. Advanced Optical Materials, 2018, 6, 1800698.	7.3	15
90	Real-time and wide-field mapping of cell-substrate adhesion gap and its evolution via surface plasmon resonance holographic microscopy. Biosensors and Bioelectronics, 2021, 174, 112826.	10.1	15

#	Article	IF	CITATIONS
91	Polarization independent and non-reciprocal absorption in multi-layer anisotropic black phosphorus metamaterials. Optics Express, 2021, 29, 21336.	3.4	15
92	Unidirectional scattering exploited transverse displacement sensor with tunable measuring range. Optics Express, 2019, 27, 4944.	3.4	15
93	Nanowires-assisted excitation and propagation of mid-infrared surface plasmon polaritons in graphene. Journal of Applied Physics, 2016, 120, .	2.5	14
94	Creation of independently controllable multiple focal spots from segmented Pancharatnam-Berry phases. Scientific Reports, 2018, 8, 9831.	3.3	14
95	Difference frequency generation in monolayer MoS ₂ . Nanoscale, 2020, 12, 19638-19643.	5.6	14
96	Fano resonance from a one-dimensional topological photonic crystal. APL Photonics, 2021, 6, 086105.	5.7	14
97	Fano resonance with high local field enhancement under azimuthally polarized excitation. Scientific Reports, 2017, 7, 1049.	3.3	13
98	Optical Heterodyne Microvibration Detection Based on All-Fiber Acousto-Optic Superlattice Modulation. Journal of Lightwave Technology, 2017, 35, 3821-3824.	4.6	13
99	Highâ€Performance Volatile Organic Compounds Microsensor Based on Few‣ayer MoS ₂ â€Coated Photonic Crystal Cavity. Advanced Optical Materials, 2018, 6, 1700882.	7.3	13
100	Measurement of full polarization states with hybrid holography based on geometric phase. Optics Express, 2019, 27, 7968.	3.4	13
101	Tightly autofocusing beams: an effective enhancement of longitudinally polarized fields. Optics Letters, 2020, 45, 575.	3.3	13
102	Azimuthal vector beam exciting silver triangular nanoprisms for increasing the performance of surface-enhanced Raman spectroscopy. Photonics Research, 2019, 7, 1447.	7.0	13
103	Electrically Tunable Second Harmonic Generation in Atomically Thin ReS ₂ . ACS Nano, 2022, 16, 6404-6413.	14.6	13
104	Self-frequency-conversion nanowire lasers. Light: Science and Applications, 2022, 11, 120.	16.6	13
105	Dynamically measuring unstable reaction–diffusion process by using digital holographic interferometry. Optics and Lasers in Engineering, 2014, 57, 1-5.	3.8	12
106	Dual-wavelength common-path digital holographic microscopy for quantitative phase imaging of biological cells. Optical Engineering, 2017, 56, 111712.	1.0	12
107	Wavelength-multiplexing surface plasmon holographic microscopy. Optics Express, 2018, 26, 13549.	3.4	12
108	Grating-assisted coupling enhancing plasmonic tip nanofocusing illuminated via radial vector beam. Nanophotonics, 2019, 8, 2303-2311.	6.0	12

#	Article	IF	CITATIONS
109	Axially Tailored Light Field by Means of a Dielectric Metalens. Physical Review Applied, 2020, 14, .	3.8	12
110	Augmenting photoluminescence of monolayer MoS ₂ using high order modes in a metal dimer-on-film nanocavity. Photonics Research, 2021, 9, 501.	7.0	12
111	Accurate and rapid measurement of optical vortex links and knots. Optics Letters, 2019, 44, 3849.	3.3	12
112	Tunable Fano-like resonance enabled by coupling a microsphere with a fiber Mach–Zehnder interferometer. Applied Optics, 2016, 55, 5756.	2.1	11
113	Physical vapor deposition of large-scale PbSe films and its applications in pulsed fiber lasers. Nanophotonics, 2020, 9, 2367-2375.	6.0	11
114	Giant All-Optical Modulation of Second-Harmonic Generation Mediated by Dark Excitons. ACS Photonics, 2021, 8, 2320-2328.	6.6	11
115	Stable loosely bounded asymmetric soliton molecules in fiber lasers. Physical Review A, 2021, 104, .	2.5	11
116	Observation of optical vortex knots and links associated with topological charge. Optics Express, 2021, 29, 38849-38857.	3.4	11
117	Continuous-wave pumped frequency upconversions in an InSe-integrated microfiber. Optics Letters, 2021, 46, 733.	3.3	10
118	Soliton metamorphosis dynamics in ultrafast fiber lasers. Physical Review A, 2021, 103, .	2.5	10
119	Complex refractive index measurement for atomic-layer materials via surface plasmon resonance holographic microscopy. Optics Letters, 2019, 44, 2982.	3.3	10
120	Selective excitation of a three-dimensionally oriented single plasmonic dipole. Photonics Research, 2019, 7, 693.	7.0	10
121	Second harmonic generation in a hollow-core fiber filled with GaSe nanosheets. Science China Information Sciences, 2022, 65, 1.	4.3	10
122	Modulation of orbital angular momentum on the propagation dynamics of light fields. Frontiers of Optoelectronics, 2019, 12, 69-87.	3.7	9
123	Selective Remote-Excitation of Gap Mode in Metallic Nanowire-Nanoparticle System Using Chiral Surface Plasmon Polaritons. IEEE Journal of Quantum Electronics, 2020, 56, 1-6.	1.9	9
124	Controlling Resonance Lineshapes of a Side-Coupled Waveguide-Microring Resonator. Journal of Lightwave Technology, 2020, 38, 4429-4434.	4.6	9
125	Optical vortex knots and links via holographic metasurfaces. Advances in Physics: X, 2021, 6, .	4.1	9
126	Unveiling radial breathing mode in a particle-on-mirror plasmonic nanocavity. Nanophotonics, 2022, 11, 487-494.	6.0	9

#	Article	IF	CITATIONS
127	High-responsivity MoS2 hot-electron telecom-band photodetector integrated with microring resonator. Applied Physics Letters, 2022, 120, .	3.3	9
128	Managing focal fields of vector beams with multiple polarization singularities. Applied Optics, 2016, 55, 9049.	2.1	8
129	Integrated digital holographic microscopy based on surface plasmon resonance. Optics Express, 2018, 26, 25437.	3.4	8
130	Few-Layer Graphene Integrated Tilted Fiber Grating For All-Optical Switching. Journal of Lightwave Technology, 2021, 39, 1477-1482.	4.6	8
131	Dynamically measuring the holo-information of light fields in three-dimensional space using a periodic polarization-structured light. Science China: Physics, Mechanics and Astronomy, 2021, 64, 1.	5.1	8
132	On-demand light wave manipulation enabled by single-layer dielectric metasurfaces. APL Photonics, 2021, 6, .	5.7	8
133	Symmetry selective cladding modes coupling in ultrafast-written fiber Bragg gratings in two-mode fiber. Optics Express, 2019, 27, 18410.	3.4	8
134	Metasurface-assisted multidimensional manipulation of a light wave based on spin-decoupled complex amplitude modulation. Optics Letters, 2022, 47, 353.	3.3	8
135	Plasmon-enhanced photoluminescence from MoS ₂ monolayer with topological insulator nanoparticle. Nanophotonics, 2022, 11, 995-1001.	6.0	8
136	High-Efficiency Second-Harmonic and Sum-Frequency Generation in a Silicon Nitride Microring Integrated with Few-Layer GaSe. ACS Photonics, 2022, 9, 1671-1678.	6.6	8
137	Miniaturized fiber Fabry-Pérot interferometer for strain sensing. Microwave and Optical Technology Letters, 2016, 58, 1510-1514.	1.4	7
138	Sparse-view imaging of a fiber internal structure in holographic diffraction tomography via a convolutional neural network. Applied Optics, 2021, 60, A234.	1.8	7
139	Periodic attraction and repulsion within the tight-bound π-phase soliton molecule. Optics Letters, 2021, 46, 5599.	3.3	7
140	Internal dynamics in bound states of unequal solitons. Optics Letters, 2022, 47, 1618.	3.3	7
141	Ultrafast Lasers: Graphene Actively Mode-Locked Lasers (Adv. Funct. Mater. 28/2018). Advanced Functional Materials, 2018, 28, 1870194.	14.9	6
142	Lowâ€Power Continuousâ€Wave Second Harmonic Generation in Semiconductor Nanowires. Laser and Photonics Reviews, 2018, 12, 1800126.	8.7	6
143	Fano-Like Resonance in an All-in-Fiber Structure. IEEE Photonics Journal, 2019, 11, 1-7.	2.0	6
144	A method for fast and robustly measuring the state of polarization of arbitrary light beams based on Pancharatnam-Berry phase. Journal of Applied Physics, 2019, 126, .	2.5	6

#	Article	IF	CITATIONS
145	Real-Time Target Detection in Visual Sensing Environments Using Deep Transfer Learning and Improved Anchor Box Generation. IEEE Access, 2020, 8, 193512-193522.	4.2	6
146	Visible frequency broadband dielectric metahologram by random Fourier phase-only encoding. Science China: Physics, Mechanics and Astronomy, 2021, 64, 1.	5.1	6
147	Flexible trajectory control of Bessel beams with pure phase modulation. Optics Express, 2022, 30, 25661.	3.4	6
148	Symmetry-breaking diffraction and dynamic self-trapping in optically induced hexagonal photonic lattices. Applied Physics Letters, 2012, 100, 061907.	3.3	5
149	Carbon nanotube-deposited tilted fiber Bragg grating for refractive index and temperature sensing. IEEE Photonics Technology Letters, 2016, , 1-1.	2.5	5
150	All-optically controlled slow and fast lights in graphene-coated tilted fiber Bragg grating. Applied Physics Express, 2019, 12, 072010.	2.4	5
151	Phase fluctuation cancellation for coherent-detection BOTDA fiber sensors based on optical subcarrier multiplexing. Optics Letters, 2021, 46, 757.	3.3	5
152	Velocity property of an optical chain generated by the tightly focused femtosecond radially polarization pulse. Applied Optics, 2021, 60, 2380.	1.8	5
153	Dynamic strain measurement based on ultrafast Brillouin collision in the correlation domain. Optics Letters, 2021, 46, 3488.	3.3	5
154	Hybrid vector beams with non-uniform orbital angular momentum density induced by designed azimuthal polarization gradient*. Chinese Physics B, 2020, 29, 094203.	1.4	5
155	Poincaré sphere analogue for optical vortex knots. Optics Letters, 2022, 47, 313.	3.3	5
156	Electrically induced dynamic Fano-like resonance in a graphene-coated fiber grating. Photonics Research, 2022, 10, 1238.	7.0	5
157	Comparison of common-path off-axis digital holography and transport of intensity equation in quantitative phase measurement. Optics and Lasers in Engineering, 2022, 157, 107126.	3.8	5
158	A Bandwidth-Tuning Device Based on Polymer-Packaged Fiber Bragg Grating. IEEE Photonics Technology Letters, 2011, 23, 1225-1227.	2.5	4
159	<italic>In-Situ</italic> Monitoring Method for Solution Volatilization Using Tilted Fiber Bragg Grating. IEEE Sensors Journal, 2015, 15, 3000-3003.	4.7	4
160	Optimized weak measurement for spatial spin-dependent shifts at Brewster angle. Applied Physics B: Lasers and Optics, 2016, 122, 1.	2.2	4
161	Dual-channel illumination surface plasmon resonance holographic microscopy for resolution improvement. Optics Letters, 2021, 46, 1604.	3.3	4
162	Co-located angularly offset fiber Bragg grating pair for temperature-compensated unambiguous 3D shape sensing. Applied Optics, 2021, 60, 4185.	1.8	4

Jianlin Zhao

#	Article	IF	CITATIONS
163	Nanometric displacement sensor with a switchable measuring range using a cylindrical vector beam excited silicon nanoantenna. Optics Express, 2021, 29, 25109.	3.4	4
164	Plasmonic Fano-like resonance in double-stacked graphene nanostrip arrays. Journal of the Optical Society of America B: Optical Physics, 2022, 39, 843.	2.1	4
165	Light-field focusing and modulation through scattering media based on dual-polarization-encoded digital optical phase conjugation. Optics Letters, 2022, 47, 2738.	3.3	4
166	Simultaneous measurement of near-water-film air temperature and humidity fields based on dual-wavelength digital holographic interferometry. Optics Express, 2022, 30, 17278.	3.4	4
167	Strong cladding mode excitation in ultrathin fiber inscribed Bragg grating with ultraviolet photosensitivity. Optics Express, 2022, 30, 25936.	3.4	4
168	Visual and dynamical measurement of Rayleigh-Benard convection by using fiber-based digital holographic interferometry. Journal of Applied Physics, 2012, 112, 113113.	2.5	3
169	Investigation of the fiber <scp>B</scp> ragg grating inscribed in multimode fiber by femtosecond laser. Microwave and Optical Technology Letters, 2017, 59, 214-219.	1.4	3
170	Formation and Evolution of Soliton in Two-Mode Fiber Laser. IEEE Photonics Journal, 2020, 12, 1-8.	2.0	3
171	Temperature-compensated fiber directional-bend sensor based on a sandwiched MMF–PMPCF structure. Applied Optics, 2021, 60, 433.	1.8	3
172	Realization and Modulation of Fano-Like Lineshape in Fiber Bragg Gratings. Journal of Lightwave Technology, 2021, 39, 4419-4423.	4.6	3
173	Nanofocusing of a metallized double periodic arranged nanocone array for surface-enhanced Raman spectroscopy. Optics Express, 2021, 29, 28086.	3.4	3
174	Tightly focused light field with controllable pure transverse polarization state at the focus. Optics Letters, 2020, 45, 6034.	3.3	3
175	Subdiffraction Focusing Metalens Based on the Depletion of Bessel Beams. IEEE Photonics Journal, 2022, 14, 1-5.	2.0	3
176	Simultaneous Control of Plasmon-Exciton and Plasmon-Trion Couplings in an Au Nanosphere and Monolayer WS2 Hybrid System. APL Photonics, 0, , .	5.7	3
177	Topological Insulator Plasmonics and Enhanced Light-Matter Interactions. Lecture Notes in Nanoscale Science and Technology, 2022, , 89-116.	0.8	3
178	Mid-wave infrared planar optical device via femtosecond laser ablation on sulfur-based polymeric glass surface. Optical Materials Express, 0, , .	3.0	3
179	Polarization-switchable nanoripples fabricated on a silicon surface by femtosecond-laser-assisted nanopatterning. Applied Optics, 2020, 59, 7211.	1.8	2
180	Measurement of thermal effect in laser pumped silicon employing infrared digital holographic interferometry. Optics Express, 2019, 27, 9439.	3.4	2

#	Article	IF	CITATIONS
181	Integration of topological insulator nanogap with atomic single layer for boosting photoluminescence. Optical Materials, 2021, 122, 111786.	3.6	2
182	Object-independent tilt detection for optical sparse aperture system with large-scale piston error via deep convolution neural network. Optics Express, 2021, 29, 41670.	3.4	2
183	Femtosecond laser plasmonic nano-printing metasurfaces for multiple-dimensional manipulation of light fields. Optics Letters, 2022, 47, 2290.	3.3	2
184	Tightly autofocusing beams along the spherical surface. Optics Express, 2022, 30, 26192.	3.4	2
185	2D MoTe ₂ : Linear Dichroism and Nondestructive Crystalline Identification of Anisotropic Semimetal Few‣ayer MoTe ₂ (Small 44/2019). Small, 2019, 15, 1970239.	10.0	1
186	Measurement of thermal effect in high-power laser irradiated liquid crystal device using digital holographic interferometry. Applied Physics B: Lasers and Optics, 2019, 125, 1.	2.2	1
187	Femtosecond laser-induced spatial-frequency-shifted nanostructures by polarization ellipticity modulation. Optics Express, 2021, 29, 29766.	3.4	1
188	Ferroelectric liquid crystal Pancharatnam-Berry lens with a fast control of output light's polarization-handedness. Optics Express, 2021, 29, 27472.	3.4	1
189	Compact Polarization-resolved Common-path Digital Holography based on Pancharatnam-Berry Phase. Optics Letters, 2021, 46, 5862-5865.	3.3	1
190	Dual-wavelength surface plasmon resonance holographic microscopy for simultaneous measurements of cell adhesion gap and cytoplasm refractive index. Optics Letters, 2022, 47, 2306-2309.	3.3	1
191	High-resolution surface plasmon resonance holographic microscopy based on symmetrical excitation. Optics and Lasers in Engineering, 2022, 153, 107000.	3.8	1
192	Manipulation of infrared light in graphene nanostructures. , 2016, , .		0
193	Polarization modulation based on graphene-integrated Ex-TFG in thin-cladding fibre. , 2017, , .		0
194	Plasmonic Manipulation and Applications in Nanostructures/Nanomaterials. , 2018, , .		0
195	10.1063/5.0053812.1.,2021,,.		0
196	Dispersion Characteristic of Spatiotemporal Sharply Autofocused Vector Airy-Circular Airy Gaussian Vortex Wave Packets. Frontiers in Physics, 2021, 9, .	2.1	0
197	Metallic nanosphere-assisted coupling ultrafast surface plasmon polaritons background-free tip nanofocusing. Optics Letters, 2021, 46, 5554-5557.	3.3	0
198	Tip-enhanced four-wave mixing internally illuminated by ultrafast vector light field. Optics Letters, 2022, 47, 1037-1040.	3.3	0

#	Article	IF	CITATIONS
199	Ferroelectric Liquid Crystal Compound Lens Based on Pancharatnam–Berry Phase. Crystals, 2022, 12, 231.	2.2	0